

Rubber toughening of polyamides with functionalized block copolymers: 1. Nylon-6

A. J. Oshinski, H. Keskkula and D. R. Paul

Department of Chemical Engineering and Center for Polymer Research, The University of Texas at Austin, Austin, Texas 78712, USA

(Received 17 August 1990; accepted 2 November 1990)

The toughening of nylon-6 using triblock copolymers of the type styrene-(ethylene-co-butylene)-styrene (SEBS) and a maleic anhydride (MA) functionalized version (SEBS-*g*-MA) is examined and compared with a conventional maleated ethylene/propylene elastomer. The changes in rheology, adhesion, crystallinity, morphology and mechanical behaviour associated with the reaction of the anhydride with the nylon-6 are documented. Combinations of the SEBS and SEBS-*g*-MA elastomer blends with nylon-6 give higher levels of toughening than is achieved with the functionalized elastomer alone. The particles of pure SEBS were about 5 μm in diameter (too large for toughening nylon-6), whereas SEBS-*g*-MA alone yielded particles of about 0.05 μm (apparently too small for optimal toughening). Combinations of the two types of elastomers gave a continuously varying particle size between these extreme limits. This suggests that the two rubbers form essentially a single population of mixed rubber particles. The order of mixing did not significantly affect the mechanical properties of these ternary blends. The evidence for maximum and minimum rubber particle sizes that can be effective for toughening nylon-6 is discussed.

(Keywords: nylon-6; blends; block copolymers; rubber toughening; maleic anhydride)

INTRODUCTION

Improvement in toughness of rigid polymers by blending with suitable elastomeric materials is widely practised and continues to be of considerable scientific interest¹⁻⁴. There are many variables that influence the degree of toughening achieved⁵ and a diversity of opinion exists about underlying mechanisms⁶⁻¹³. However, there is general agreement that the morphology of the blend or more specifically the rubber particle size is an influential factor; but its influence may vary widely from one system to another. The optimal size appears to depend on the deformation mechanisms involved⁸ and possibly other factors. For example, it is generally recognized that rubber particles must be larger than about 1 μm for toughening of polystyrene^{5,14-17}, whereas for nylon-6 or nylon-6,6 the particles must be generally smaller than 1 μm ^{2,18,19}. For polyamides, there is a sharp transition from tough to brittle as the particle size exceeds a certain critical value that depends on a number of factors including rubber content. Wu⁶ has proposed that it is the distance between particles rather than their size which is the most fundamental parameter controlling the toughening of polyamides. It is also recognized that some degree of adhesion or coupling of the rubber and matrix phases must exist, and hydrocarbon elastomers do not have sufficient affinity for polar polymers like polyamides, polyesters, etc. This problem has been solved by incorporating functional groups into the elastomer that can react with condensation type polymers like the polyamides^{2,4,6-8,19,20}. Such grafting processes provide the adhesion needed and dramatically affect the ability to disperse the elastomer and the resulting particle size^{18,21-24}. The most well developed example of this involves the so-called super-tough nylons, which typically

are blends of nylon-6,6 or nylon-6 containing an ethylene/propylene elastomer that has been grafted with maleic anhydride (MA)^{2,7,19,21,25,26}.

In this paper, we present results on toughening of nylon-6 by blending with a styrene-butadiene-styrene triblock copolymer whose mid-block has been hydrogenated and resembles an ethylene/butene copolymer. Thus, the base copolymer is designated as styrene-(ethylene-co-butylene)-styrene (SEBS) and the maleated version as SEBS-*g*-MA. Such triblock copolymers are thermoplastic elastomers that can flow at high temperature but have properties of crosslinked rubber at low temperature²⁷. These materials and their use as impact modifiers have been described by Modic *et al.*²⁸⁻³⁰, and this work elaborates on some of their observations. We examine here the mechanical properties of blends of nylon-6 with SEBS-*g*-MA and SEBS copolymers including ternary compositions and the importance of order of mixing the components together. The blends were characterized by measurements of melt rheology, interfacial adhesion, heat of fusion of nylon, dynamic mechanical behaviour and transmission electron microscopy. We also briefly compare the effectiveness for toughening nylon-6 of this block copolymer system with that of a typical functionalized ethylene/propylene copolymer system. Use of combinations of functionalized and unfunctionalized rubber proves to be a very effective way of controlling particle size and hence blend properties^{24,28-32}. The results of this work confirm the existence of an upper limit on the size of elastomer particles that can give super-tough nylon-6 blends, and it also suggests that there is a lower size limit for toughening of nylon-6³³.

An accompanying paper reports on a similar study using nylon-6,6 as the matrix.

Table 1 Materials used

Designation used here	Material (commercial designation)	Composition	Molecular weight	Relative melt viscosity ^a	Source
Nylon-6	(Capron 8207F)		$\bar{M}_n = 25\,000$	1.00	Allied-Signal Inc.
SEBS	Styrene/ethylene-butene/styrene (Kraton G 1652)	29% styrene	Styrene block = 7000 EB block = 37 500	1.79	Shell Chemical Co.
SEBS- <i>g</i> -MA	Styrene/ethylene-butene/styrene (Kraton G 1901X)	29% styrene 1.84 wt% MA ^b	Not available	1.16	Shell Chemical Co.
SEBS-H	Styrene/ethylene-butene/styrene (Kraton G 1651)	29% styrene	Styrene block = 29 000 EB block = 116 000	See text	Shell Chemical Co.
EPM- <i>g</i> -MA	Ethylene/propylene rubber grafted with maleic anhydride	1.2 wt% MA	$M_n = 40\,000\text{--}50\,000$	2.59	COPOLYMER Co.

^aBrabender torque at 240°C and 60 r.p.m. divided by that of nylon-6

^bDetermined by elemental analysis after solvent/non-solvent purification

MATERIALS AND PROCEDURES

Table 1 summarizes the sources and some pertinent characteristic information about the materials used in this study. The nylon-6 used is a commercially available polymer having $\bar{M}_n = 25\,000$ and approximately 40 mmol kg⁻¹ each of carboxyl and amine groups. Owing to its hygroscopic nature, all materials containing nylon-6 were dried at 80°C for at least 12 h in a vacuum oven to remove sorbed water before processing.

Four rubbers were employed, two of which were maleated. The triblock copolymers have styrene end-blocks and a hydrogenated butadiene mid-block resembling an ethylene/butene copolymer. Two are similar in nature except for the molecular weights of the block segments. The higher-molecular-weight rubber is designated as SEBS-H and the lower one as SEBS. The third SEBS type copolymer was grafted with 1.84% by weight maleic anhydride (determined by elemental analysis) along the olefinic mid-block and is designated as SEBS-*g*-MA. This material is most similar to the lower-molecular-weight copolymer, SEBS. The third type of rubber investigated was an ethylene-propylene monomer-*graft*-maleic anhydride (EPM-*g*-MA) having 1.2% by weight bound maleic anhydride. The two functionalized rubbers have the potential of reacting with nylon-6 through the terminal amine groups or possibly via the amide linkages to form imide linkages.

For rheological studies, the various polymers were mixed in a Brabender Plasticorder at 60 r.p.m. using a 50 ml mixing head with standard rotors while the torque was recorded. All tests using nylon-6 were made at 240°C except where noted otherwise.

Blends prepared for mechanical testing were melt mixed using a Killion single-screw extruder ($L/D = 30$; 1 inch (2.54 cm) diameter) at a screw speed of 40 r.p.m. The temperature of the barrel and the die was set at 240°C for all compositions containing nylon-6. A temperature of 180°C was used to blend the functionalized and unfunctionalized copolymers with each other. A single 1/8 inch (0.318 cm) strand was extruded, quenched in a water bath and pelletized. All blends were extruded twice to ensure adequate mixing and/or reaction. The extruded material was then injection moulded into standard tensile (ASTM D638 type I) and Izod (ASTM D256) bars (1/8 inch (0.318 cm) thick) using an Arburg Allrounder screw injection moulding machine. Detailed conditions for all processing operations are provided elsewhere³⁴.

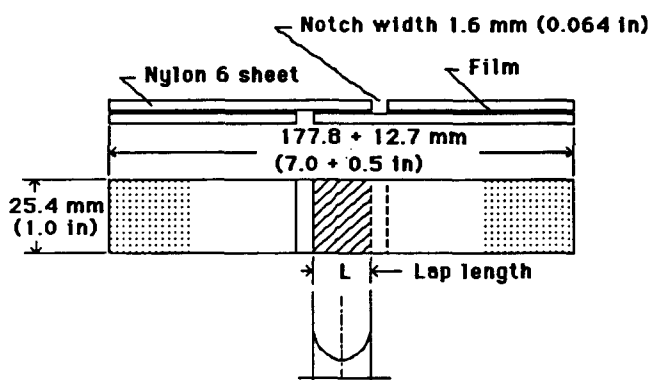


Figure 1 Schematic illustration of a lap shear specimen for adhesion measurements ($L = 1.27$ cm used here)

Injection-moulded test samples were visually inspected for air bubbles, and those which contained such defects were discarded. After inspection, the samples were placed in a sealed plastic bag inside a desiccator to prevent water sorption. Thus, the samples were tested at 'dry as-moulded' conditions. Tensile testing was performed on an Instron in accordance with ASTM D638 using a crosshead speed of 2.0 inch min⁻¹ (5.08 cm min⁻¹). An extensometer strain gauge with a 2 inch (5.08 cm) gap was used to obtain the modulus and yield strain values. Elongation at break was determined by the crosshead travel rate assuming a gauge length of 9.65 cm. Izod testing was conducted using ASTM D256 method A with 1/8 inch (0.318 cm) thick specimens at room temperature.

Lap shear adhesion specimens were prepared by using nylon-6 outer layers compression moulded at 240°C at 1.72 GPa into 8 inch × 8 inch × 1/8 inch (20.3 cm × 20.3 cm × 0.318 cm) plaques. The inner rubber layer was also compression moulded using a frame thickness of 0.08 cm. A sandwich of two nylon-6 outer layers and a rubber film middle layer were then laminated together in a frame mould at 240°C and 1.72 GPa for 10 min followed by cooling to room temperature by circulating water through the mould platens. Final test specimens were cut according to ASTM D3165 as shown in Figure 1. Specimens that contained defects in the lap area were rejected. The specimens were pulled at 0.508 cm min⁻¹ and the load at which adhesive failure of the joint occurred was recorded. This force divided by the lap area is the adhesion strength reported here.

Thermal and dynamic mechanical tests were performed on the blends to monitor changes in morphology and

transitional behaviour relative to the pure components that may result from grafting reaction between nylon-6 and SEBS-*g*-MA. Heats of fusion for the blends were measured using a differential scanning calorimeter (Perkin-Elmer DSC-7) with a scan rate of 20°C min⁻¹ and a hold time of 0.5 min at the end of each heating and cooling period. D.s.c. samples were taken from injection-moulded bars and were given two successive heating ramps. The heat of fusion of nylon-6 was defined as the area under the endothermic peak between the temperatures 130 and 240°C. Tan δ and loss modulus E'' were measured using a Polymer Laboratories Inc. dynamic mechanical thermal analyser (DMTA Mark I) at a frequency of 1 Hz. The blends were cooled to -100°C using liquid nitrogen and heated at a rate of 2°C min⁻¹ to at least 160°C. All transition temperatures reported in this study were calculated by the DMTA software.

The morphology of selected blends was examined for us by an industrial laboratory using transmission electron microscopy (TEM). Samples were cryogenically microtomed from injection-moulded bars and stained with OsO₄ and RuO₄. All photomicrographs were taken at a magnification of 25 000 \times .

RHEOLOGY

The importance of rheology in the current context is two-fold. First, the rheological properties of the individual components influence the morphological structure of the product formed during processing. Accordingly, it is essential to provide characteristic information on each material at the processing conditions used³⁵⁻³⁸. Secondly, a chemical reaction between the components of the type expected here should lead to an increase in the viscosity of the mixture relative to that without any reaction. As a first approximation, the latter is given by a composition-weighted average of the individual component properties. Therefore, rheological measurements can be used as a means for demonstrating the occurrence of reactions in functionalized systems³⁹⁻⁴².

In order to assess reaction effects, it is necessary to obtain relative viscosities of all individual components to construct the non-reactive baseline. As seen in *Figure 2*, neat nylon-6 reaches a steady-state torque level after approximately 5 min in the Brabender at 240°C. During the first 5 min or so, heating of the cold polymer pellets and fluxing dominate the response, but after this non-isothermal transient, the torque begins to level off. However, at 280°C the torque continues to decline with time probably because of some degradation at this high temperature.

Similar results are shown in *Figure 3* for SEBS and SEBS-*g*-MA. For comparable conditions, the non-functional SEBS is more viscous than nylon-6 and SEBS-*g*-MA. The functionalized rubber, SEBS-*g*-MA, is slightly more viscous than nylon-6. These materials all show some decrease in torque with time, which may reflect gradual degradation at these conditions.

To alter the effective level of the maleic anhydride functional groups in the rubber phase in the blends with nylon-6, SEBS and SEBS-*g*-MA rubbers were blended together in various ratios. *Figure 4* shows that the Brabender torque for mixtures of the two rubbers conforms reasonably well to an additive relation as expected for a non-reactive system. *Figure 5* contrasts the

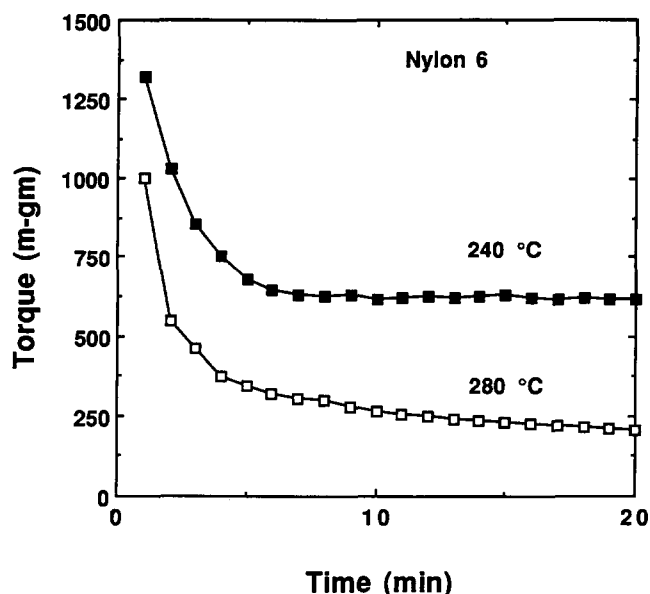


Figure 2 Brabender torque response for nylon-6 at 240 and 280°C at 60 r.p.m.

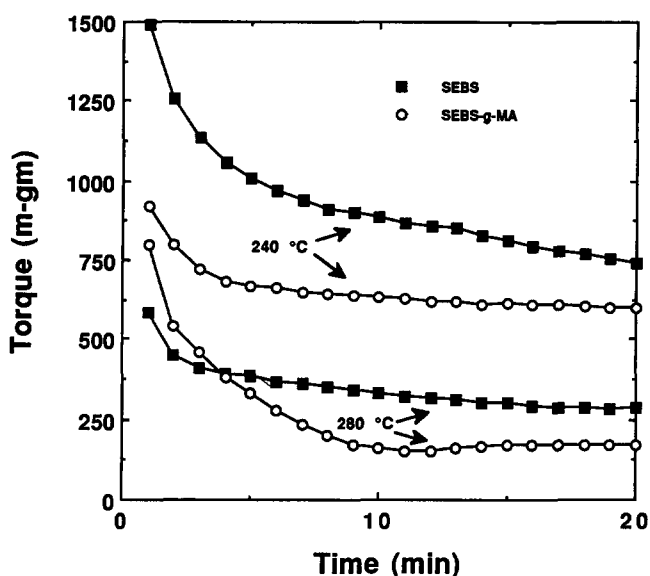


Figure 3 Brabender torque response for SEBS and SEBS-*g*-MA at 240 and 280°C at 60 r.p.m.

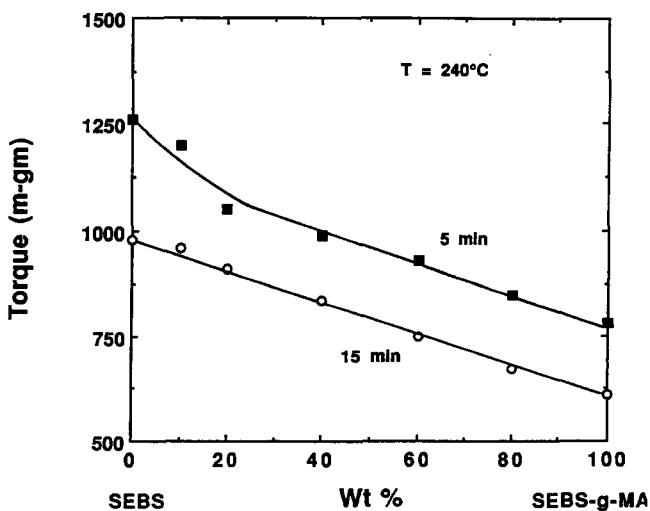


Figure 4 Brabender torque for SEBS/SEBS-*g*-MA blends with mixing time as a parameter at 240°C and 60 r.p.m.

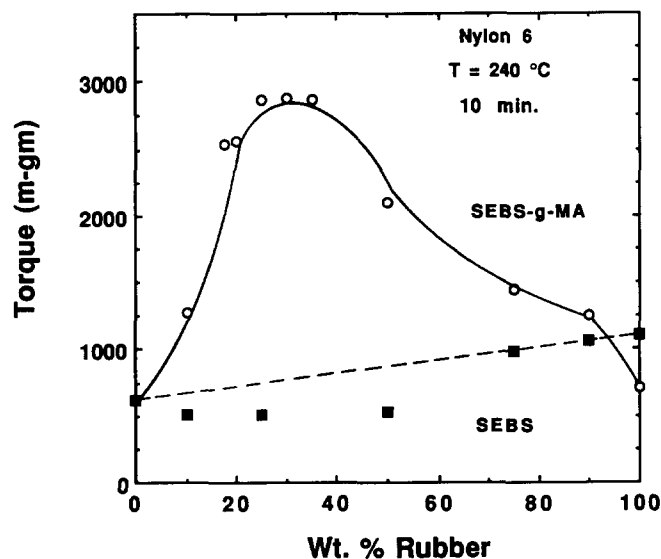


Figure 5 Brabender torque for blends of nylon-6 with SEBS and with SEBS-*g*-MA after 10 min at 240°C and 60 r.p.m.

torque response for blends of nylon-6 with non-functionalized and functionalized SEBS copolymers. The lower curve for SEBS does not strictly follow an additive relation since at low amounts of rubber (0–40%) the measured torque falls somewhat below the tie line connecting SEBS and nylon-6. Beyond about 60% SEBS, the measured torque falls on the tie line. This change probably reflects the phase inversion where the rubber becomes the matrix phase and nylon-6 is the dispersed phase. Nevertheless, the response is essentially additive compared to the strong maximum seen when nylon-6 is blended with SEBS-*g*-MA. Between 25 and 35% SEBS-*g*-MA, the torque reaches a maximum value. It is quite apparent that a reaction has occurred since the viscosity of the blend is about 4–5 times the level of either component. Interestingly, the maleic anhydride from the SEBS-*g*-MA and the amine groups from the nylon-6 are in stoichiometric balance at about 17.5% rubber. The significance of this needs to be examined in greater detail with materials of varying levels of functionality.

Figure 6 shows torque *versus* time responses for blends of 80% nylon-6 with 20% rubber, where the SEBS/SEBS-*g*-MA ratio is varied as shown. It is evident that blends which contain the functionalized rubber have torque levels above the additive tie line. This is a result of the graft copolymer being formed as discussed earlier. The reaction is evidently quite fast since the torque does not rise as the mixing time increases. Any reaction kinetic effect is masked within the transient fluxing period. As the SEBS-*g*-MA fraction in the rubber is increased, the overall torque level increases and there is a more rapid decline in the torque with time, which may reflect mechanical mastication of the grafted melt. At the highest levels of SEBS-*g*-MA, the melt appeared gelatinous after 20 min, indicating that the reaction was quite extensive and that further processing would only degrade the blend. Figure 7 shows that there is a simple monotonic increase in torque when the fraction that SEBS-*g*-MA contributes to the 20% total rubber is increased.

As seen in Figure 8, replacing SEBS with the higher-molecular-weight non-functionalized rubber, SEBS-H, shifts the torque levels to only slightly higher values than for the SEBS systems. The torque level of

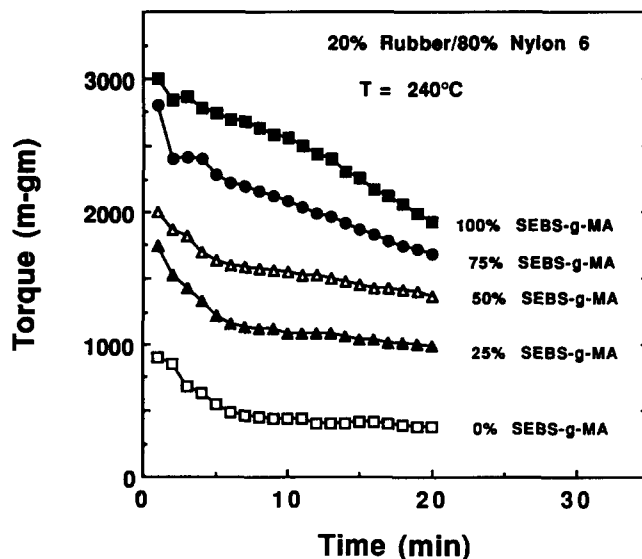


Figure 6 Brabender torque response for 20% rubber/80% nylon-6 blends for various ratios of SEBS-*g*-MA/SEBS rubbers at 240°C and 60 r.p.m.

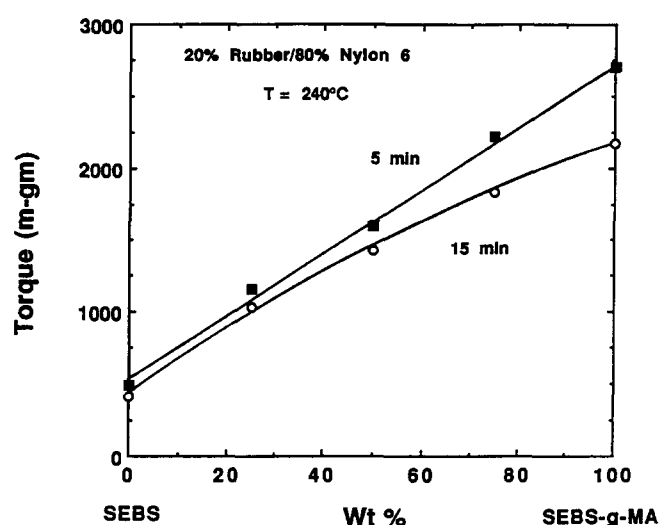


Figure 7 Brabender torque for 20% total rubber/80% nylon-6 blends as a function of SEBS-*g*-MA/SEBS ratio after 5 and 15 min at 240°C and 60 r.p.m.

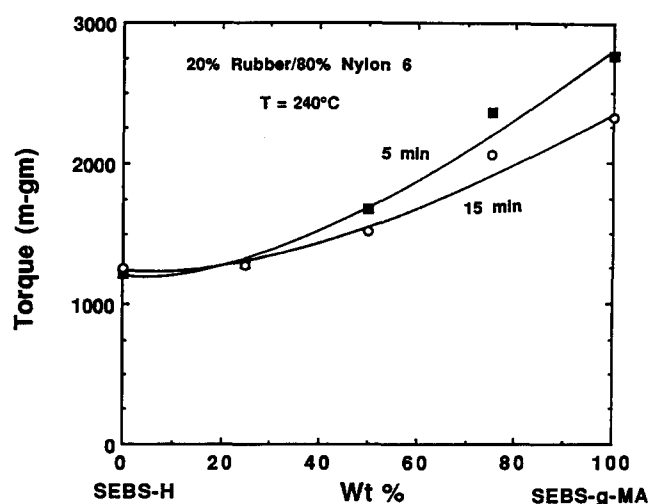


Figure 8 Brabender torque for 20% total rubber/80% nylon-6 blends as a function of SEBS-*g*-MA/SEBS-H ratio after 5 and 15 min at 240°C and 60 r.p.m.

pure SEBS-H could not be determined since this high-molecular-weight material would not flux in the mixing head and remained in a crumb-like form. Nevertheless, the torque trend for SEBS-H mixtures with SEBS-*g*-MA are similar to those for SEBS.

It is of interest to compare the use of EPM-*g*-MA with SEBS-*g*-MA blends with nylon-6. Figure 9 shows that increasing the level of SEBS-*g*-MA significantly increases the torque for the blend. The 30% concentration shows a sharp decline in torque with time. Similar results are shown in Figure 10 for varying levels of EPM-*g*-MA. The pattern of behaviour is complex and more difficult to interpret than that for SEBS-*g*-MA. There is clear evidence for reaction with the nylon-6 since the blends have significantly higher torques than do nylon-6 or EPM-*g*-MA alone. These blends exhibited a significant

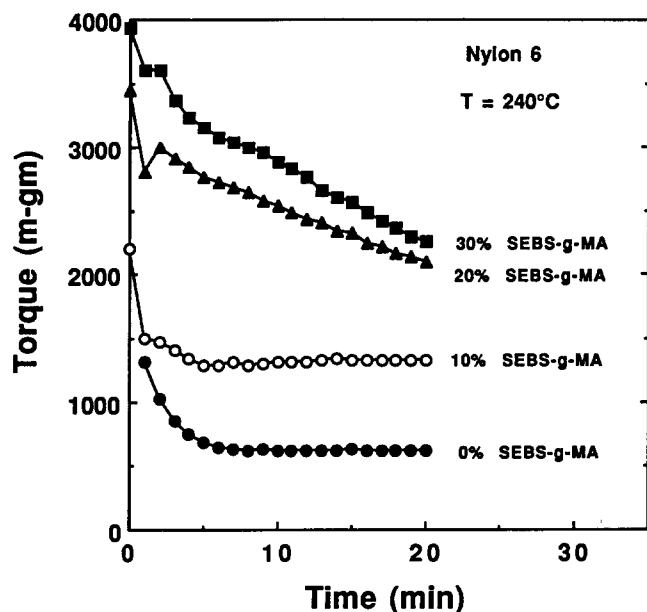


Figure 9 Brabender torque response for SEBS-*g*-MA blends with nylon-6 at 240°C and 60 r.p.m.

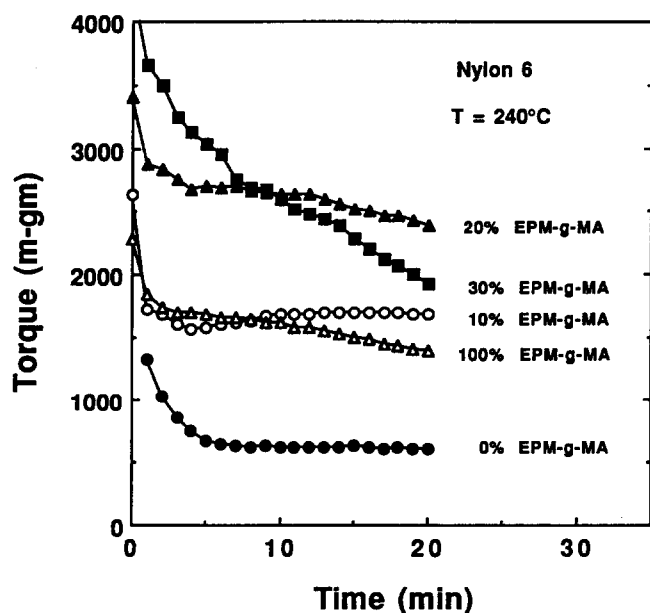


Figure 10 Brabender torque response for EPM-*g*-MA blends with nylon-6 at 240°C and 60 r.p.m.

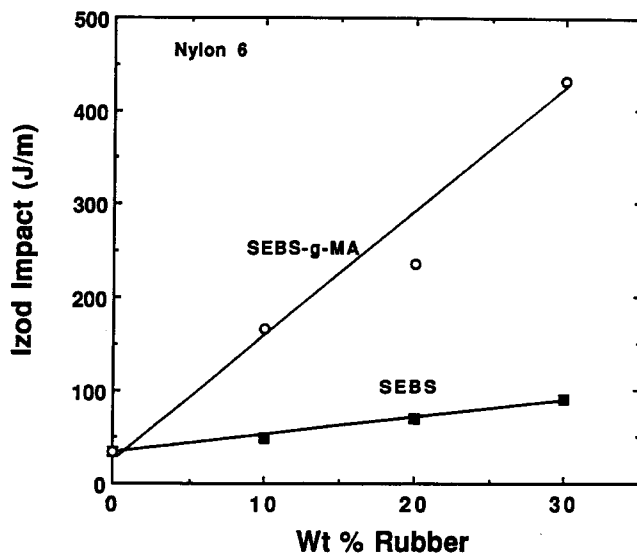


Figure 11 Notched Izod impact strength of nylon-6 blends with SEBS and with SEBS-*g*-MA

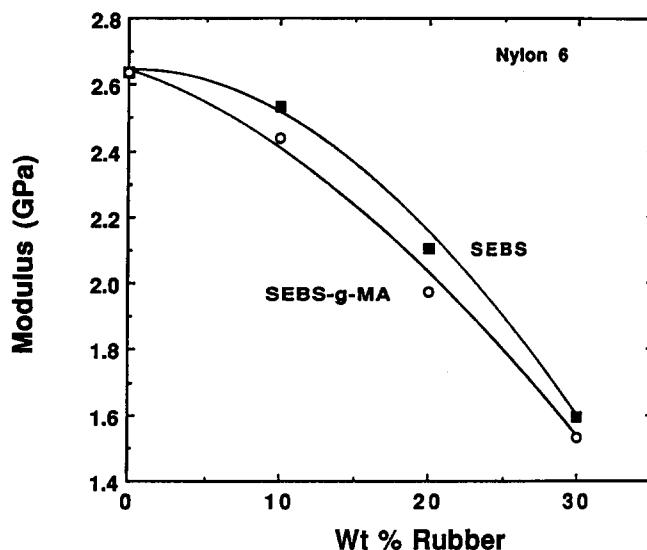


Figure 12 Tensile modulus of nylon-6 blends with SEBS and with SEBS-*g*-MA

Weissenberg-type effect where normal stresses forced as much as 10% of the material from the Brabender chamber during mixing. At high levels of SEBS-*g*-MA, similar effects were observed but to a much lesser extent than with EPM-*g*-MA. No doubt this phenomenon is at least partly responsible for the complex trends seen in Figure 10; hence, these experiments do not reflect simple viscosity responses in the case of EPM-*g*-MA blends with nylon-6.

MECHANICAL PROPERTIES

Effect of mixing order and SEBS-*g*-MA concentration

Blends of nylon-6 with varying levels of SEBS and SEBS-*g*-MA were prepared using the procedures outlined earlier. Key mechanical properties of these blends are shown in Figures 11–13. As expected, there is significant toughening when the functionalized block copolymer is added, whereas the unfunctionalized copolymer leads to only minor increases. Both types of rubber cause

decreases in both modulus and strength; and on the whole, the reductions for SEBS-*g*-MA are just slightly greater than for SEBS. However, for the maleated block copolymer alone, the levels of impact strength achieved are not as great as obtained using functionalized

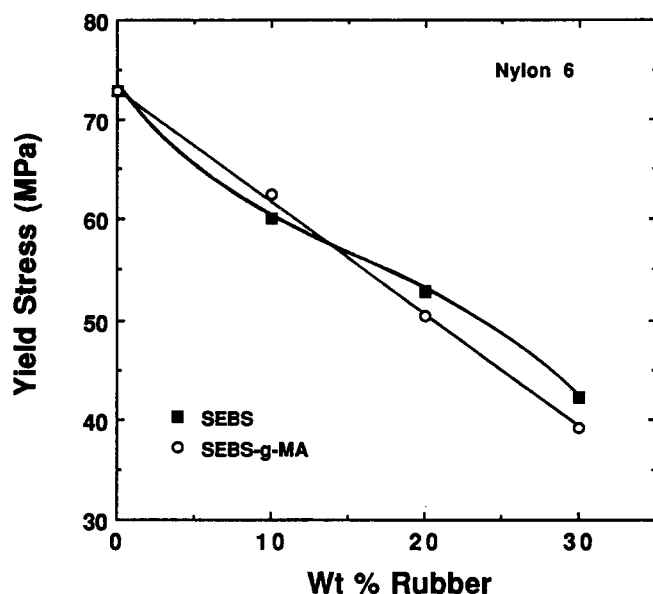


Figure 13 Tensile yield stress of nylon-6 blends with SEBS and with SEBS-*g*-MA

ethylene/propylene elastomers according to recent reports^{2,7,19,21,25,26} and as found here. Modic and coworkers²⁸⁻³⁰ have reported that super-tough blends equivalent to those found in EPM-*g*-MA systems are obtained when certain combinations of SEBS and SEBS-*g*-MA are added to nylon-6. The following experiments elaborate on this important observation.

The three materials, nylon-6, SEBS and SEBS-*g*-MA, might be combined into a ternary blend of a given composition using a variety of different mixing protocols. For example, all three components may be introduced simultaneously to the extruder or alternatively the two rubbers might be melt mixed first and then blended with nylon-6 (N6) in a second step. Here, we designate the former as N6/SEBS/SEBS-*g*-MA and the latter as SEBS/SEBS-*g*-MA + N6, i.e. a '+' denotes a second melt mixing step. Therefore for the SEBS/SEBS-*g*-MA + N6 case, there was a total of two extrusion passes for the blend. Table 2 indicates a total of five different order of mixing procedures that were used here. It is conceivable that the morphology and properties of the blend would depend on the mixing order used. The main issue is whether the functionalized rubber can compatibilize the non-functional rubber or not. That is, does each rubber particle formed contain a mixture of the two rubbers or are there two populations of particles (one for each type of rubber)? Intermediate situations may also be possible. One might expect the mixing order SEBS/SEBS-*g*-MA + N6 to be the most likely to yield one population,

Table 2 Effect of order of mixing and SEBS/SEBS-*g*-MA ratio (wt% of SEBS-*g*-MA is indicated in headings) on mechanical properties of blends containing 80% nylon-6 and 20% total rubber

(a) Izod impact ($J m^{-1}$)					
	0	25	50	75	100
N6/SEBS + SEBS- <i>g</i> -MA	69.4 ± 5	961 ± 139	614 ± 107	262 ± 37	235 ± 32
N6/SEBS- <i>g</i> -MA + SEBS	69.4 ± 5	913 ± 123	689 ± 150	315 ± 53	235 ± 32
SEBS/SEBS- <i>g</i> -MA + N6	69.4 ± 5	972 ± 123	673 ± 101	363 ± 64	235 ± 32
N6/SEBS + N6/SEBS- <i>g</i> -MA	69.4 ± 5	924 ± 96	748 ± 123	267 ± 59	235 ± 32
N6/SEBS/SEBS- <i>g</i> -MA	69.4 ± 5	951 ± 117	619 ± 80	315 ± 53	235 ± 32
(b) Modulus (MPa)					
	0	25	50	75	100
N6/SEBS + SEBS- <i>g</i> -MA	2103 ± 6	1979 ± 41	2028 ± 69	2048 ± 76	1972 ± 41
N6/SEBS- <i>g</i> -MA + SEBS	2103 ± 6	2027 ± 34	1986 ± 21	1938 ± 21	1972 ± 41
SEBS/SEBS- <i>g</i> -MA + N6	2103 ± 6	1917 ± 34	1897 ± 21	1938 ± 48	1972 ± 41
N6/SEBS + N6/SEBS- <i>g</i> -MA	2103 ± 6	1966 ± 28	1890 ± 34	1890 ± 41	1972 ± 41
N6/SEBS/SEBS- <i>g</i> -MA	2103 ± 6	1938 ± 69	1917 ± 55	1979 ± 48	1972 ± 41
(c) Elongation at break (%)					
	0	25	50	75	100
N6/SEBS + SEBS- <i>g</i> -MA	57 ± 10	247 ± 6	220 ± 11	211 ± 18	169 ± 9
N6/SEBS- <i>g</i> -MA + SEBS	57 ± 10	268 ± 39	241 ± 27	200 ± 14	169 ± 9
SEBS/SEBS- <i>g</i> -MA + N6	57 ± 10	272 ± 39	222 ± 6	226 ± 8	169 ± 9
N6/SEBS + N6/SEBS- <i>g</i> -MA	57 ± 10	256 ± 26	230 ± 13	213 ± 11	169 ± 9
N6/SEBS/SEBS- <i>g</i> -MA	57 ± 10	285 ± 35	225 ± 11	211 ± 14	169 ± 9
(d) Yield stress (MPa)					
	0	25	50	75	100
N6/SEBS + SEBS- <i>g</i> -MA	53.1 ± 0.5	50.3 ± 0.4	51.7 ± 0.5	52.4 ± 0.5	50.3 ± 0.8
N6/SEBS- <i>g</i> -MA + SEBS	53.1 ± 0.5	51.0 ± 0.3	51.7 ± 0.3	50.3 ± 0.6	50.3 ± 0.8
SEBS/SEBS- <i>g</i> -MA + N6	53.1 ± 0.5	49.7 ± 0.3	48.9 ± 0.3	51.0 ± 0.6	50.3 ± 0.8
N6/SEBS + N6/SEBS- <i>g</i> -MA	53.1 ± 0.5	49.7 ± 0.4	48.9 ± 0.3	49.2 ± 0.3	50.3 ± 0.8
N6/SEBS/SEBS- <i>g</i> -MA	53.1 ± 0.5	50.3 ± 0.3	48.9 ± 0.3	50.6 ± 0.3	50.3 ± 0.8

while the order N6/SEBS + N6/SEBS-*g*-MA might be the most likely to yield two distinct populations. In the remainder of this section, we examine the effect of mixing order and the ratio of functionalized to non-functional block copolymers on blend mechanical properties.

Table 2 shows impact and tensile properties of blends of 80% nylon-6 and 20% rubber as a function of mixing order and the fraction of the total rubber that is of the functionalized type. Standard deviations are shown for each property. Quite surprisingly, the effect of mixing order for a given overall composition is not a significant factor in determining properties when the standard deviations for individual measurements are considered. As a result of this important finding, we focus hereafter only on blends prepared by simultaneous addition of all three components owing to the considerable simplification this route offers. This apparent insensitivity to mixing order may not apply to other blend systems, however.

Table 2 also confirms that there is a maximum in toughening when a combination of SEBS and SEBS-*g*-MA are used at 20% total rubber. Table 3 shows similar trends at other levels of total rubber. To examine this point more carefully, additional blends containing a total copolymer content of 20% were prepared until this maximum was located more precisely (see Figure 14). This maximum occurs at a ratio of SEBS to SEBS-*g*-MA at about 4.3 to 1 or at an average maleic anhydride content of 0.35 wt% in the rubber phase. The Izod impact strengths achieved at this composition are equivalent to or higher than those reported for functionalized ethylene/propylene elastomers^{2,7,19,25,26}. The morphology of compositions labelled with the letters A through F are described later. Tensile properties were also determined for this series of blends containing 20% total rubber with the results shown in Figures 15–17. Strength and stiffness generally decline as more functionalized rubber is used. The average standard deviation for all compositions is shown at the 50% point for reference. The elongation at break values parallel the Izod impact results.

Table 3 Mechanical properties of nylon-6 with varying levels of total rubber and SEBS/SEBS-*g*-MA ratios^a

SEBS- <i>g</i> -MA (%)	Impact (J m ⁻¹)	Modulus (MPa)	Yield stress (MPa)	Elongation (%)
Nylon-6 Virgin	39.5 ± 9.1	2865 ± 55	80.9 ± 1.2	272 ± 31
Nylon-6 EX-2	33.6 ± 11.2	2639 ± 110	72.9 ± 0.8	90 ± 30
10% rubber				
100	166 ± 43	2437 ± 55	62.5 ± 0.6	73 ± 32
75	278 ± 85	2394 ± 90	64.7 ± 0.5	108 ± 31
50	256 ± 75	2407 ± 117	64.6 ± 0.6	133 ± 49
25	433 ± 219	2434 ± 55	64.3 ± 0.8	86 ± 49
0	48 ± 5	2532 ± 76	60.0 ± 3.2	206 ± 32
20% rubber				
100	237 ± 32	1975 ± 41	50.4 ± 0.8	169 ± 9
75	315 ± 53	1979 ± 48	50.6 ± 0.3	211 ± 14
50	619 ± 80	1917 ± 55	49.0 ± 0.3	225 ± 11
25	950 ± 117	1938 ± 69	50.3 ± 0.3	285 ± 35
0	69 ± 5	2106 ± 55	52.8 ± 0.5	57 ± 10
30% rubber				
100	432 ± 69	1531 ± 21	39.2 ± 0.4	171 ± 22
75	294 ± 27	1590 ± 28	42.0 ± 0.3	228 ± 10
50	534 ± 101	1588 ± 48	42.1 ± 0.4	238 ± 28
25	897 ± 150	1708 ± 62	43.4 ± 0.5	166 ± 50
0	91 ± 11	1593 ± 28	42.2 ± 0.5	58 ± 9

^a Blends prepared by simultaneous addition of all three materials to extruder

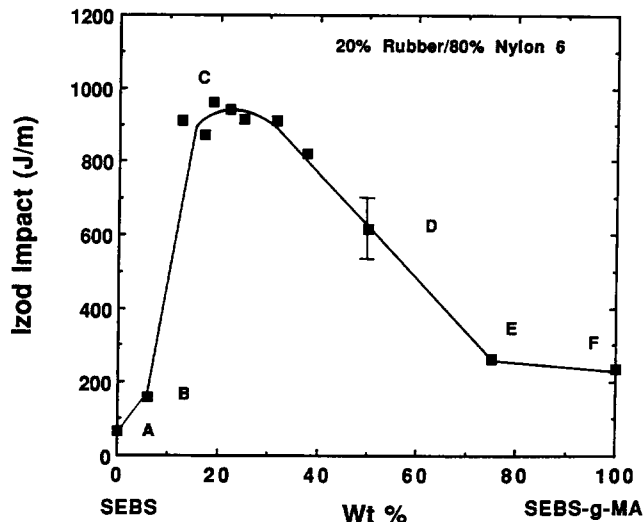


Figure 14 Notched Izod impact strength for 20% rubber/80% nylon-6 blends for various ratios of SEBS/SEBS-*g*-MA ratio. The letters A–F correspond to the photomicrographs shown in Figure 25

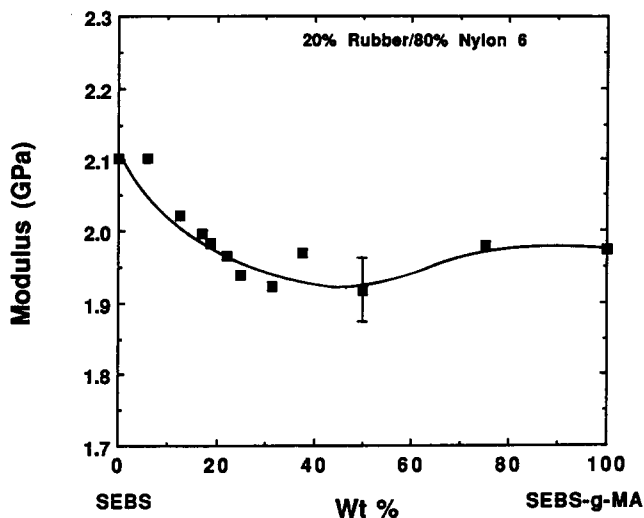


Figure 15 Tensile modulus of 20% rubber/80% nylon-6 blends as a function of SEBS/SEBS-*g*-MA ratio. The bar at 50% denotes average standard deviation for this property

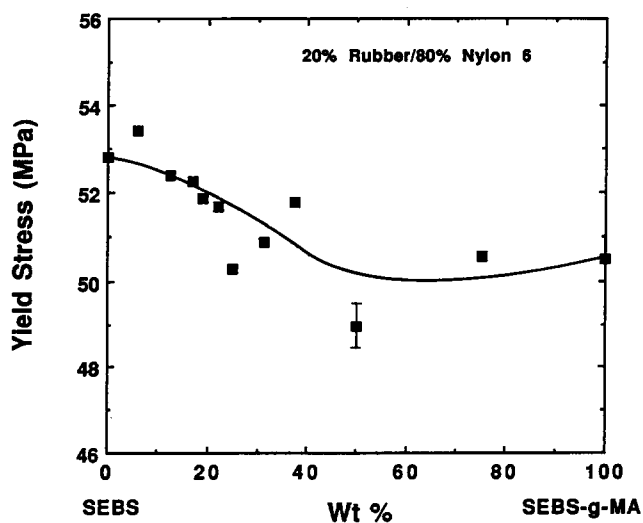


Figure 16 Tensile yield strength of 20% rubber/80% nylon-6 blends as a function of SEBS/SEBS-*g*-MA ratio. The bar at 50% denotes average standard deviation for this property

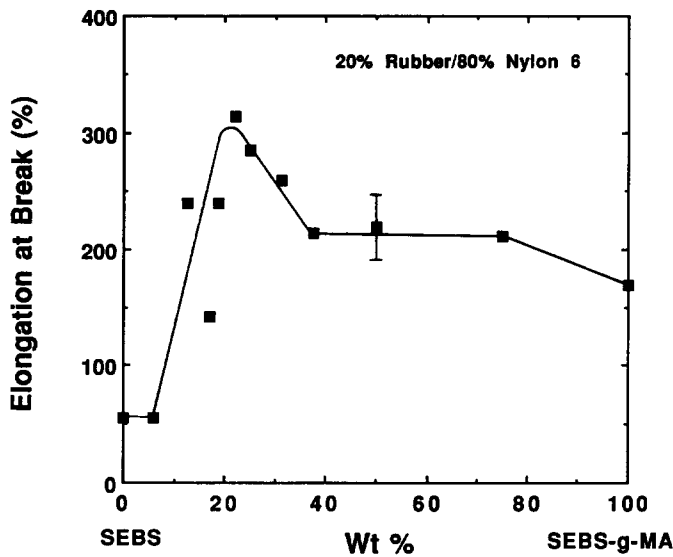


Figure 17 Elongation at break of 20% rubber/80% nylon-6 blends as a function of SEBS/SEBS-g-MA ratio. The bar at 50% denotes average standard deviation for this property

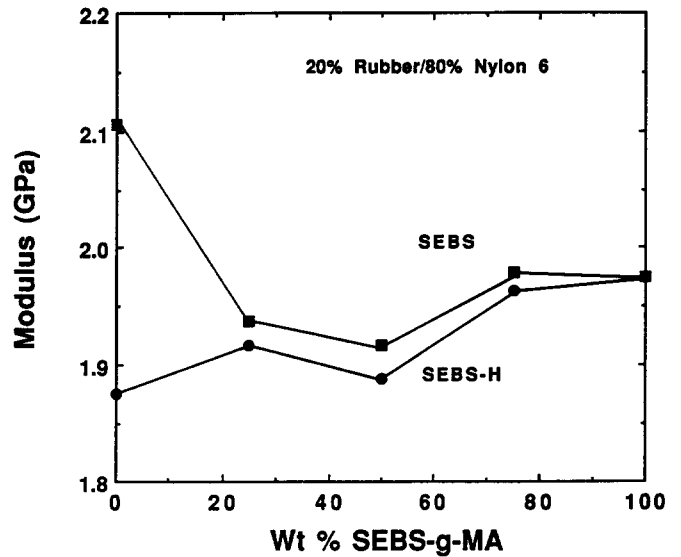


Figure 19 Tensile modulus for 20% rubber/80% nylon-6 blends as a function of the ratio of SEBS or SEBS-H non-functionalized rubber to SEBS-g-MA

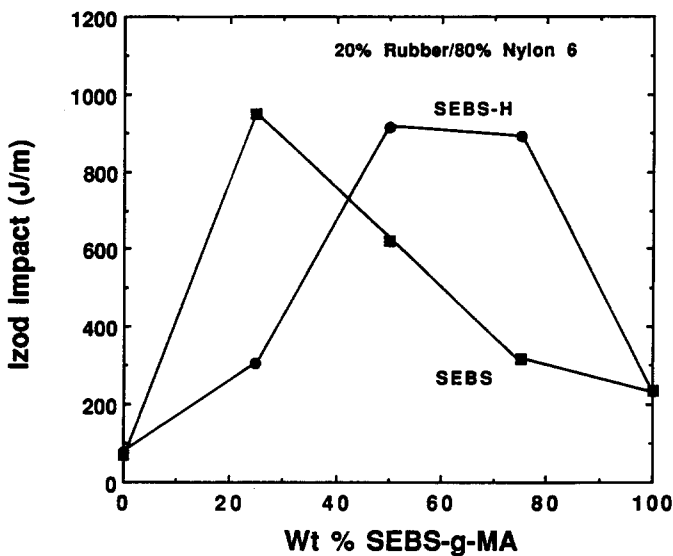


Figure 18 Notched Izod impact strength for 20% rubber/80% nylon-6 blends as a function of the ratio of SEBS or SEBS-H non-functionalized rubber to SEBS-g-MA

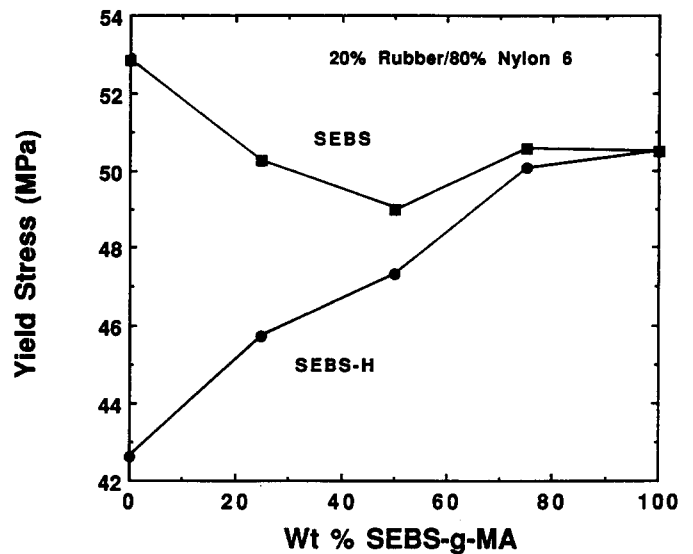


Figure 20 Tensile yield stress for 20% rubber/80% nylon-6 blends as a function of the ratio of SEBS or SEBS-H non-functionalized rubber to SEBS-g-MA

Comparison with other elastomers

For comparison, a limited examination of blends of nylon-6 with other elastomeric components was made. First, the non-functional SEBS was replaced with a higher-molecular-weight version of this copolymer, SEBS-H. As pointed out earlier it is so elastic even at 240°C that it cannot be characterized by torque rheometry. Ternary blends containing 20% total elastomer were prepared by simultaneous addition of all components, and their mechanical properties are shown in Figures 18–21. Data at the same compositions using SEBS are reproduced in these figures for comparison. There is a similar trend in impact strength for both block copolymers; however, the maximum toughening occurs at higher levels of SEBS-g-MA when the higher-molecular-weight copolymer is used. We might speculate that, owing to the more viscous nature of the latter, more functional copolymer is needed to achieve optimal

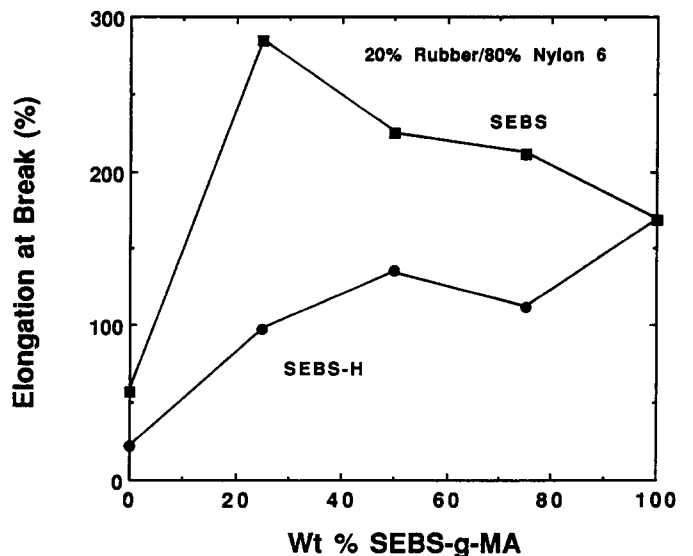


Figure 21 Elongation at break for 20% rubber/80% nylon-6 blends as a function of the ratio of SEBS or SEBS-H non-functionalized rubber to SEBS-g-MA

dispersion of the elastomer phase. As seen in Figures 19–21 all of the tensile properties are lower for blends of SEBS-H than those containing SEBS. The modulus and yield stress differences diminish as more SEBS-*g*-MA is added to the blend. In general, SEBS seems to be the preferred non-reactive elastomer for this use.

Finally, we compared how the properties of nylon-6 are changed by blending with functionalized ethylene/propylene rubber, EPM-*g*-MA, relative to SEBS-*g*-MA. Figure 22 shows that the impact strength, at a given rubber level, is always higher for the EPM-*g*-MA than for SEBS-*g*-MA (no SEBS present). As seen in Figure 23, the blend modulus is not decreased as much by addition of SEBS-*g*-MA as when EPM-*g*-MA is used. This seems reasonable since 29% of the block copolymer is hard polystyrene domains which elevate the modulus of this elastomer relative to ethylene/propylene materials, which

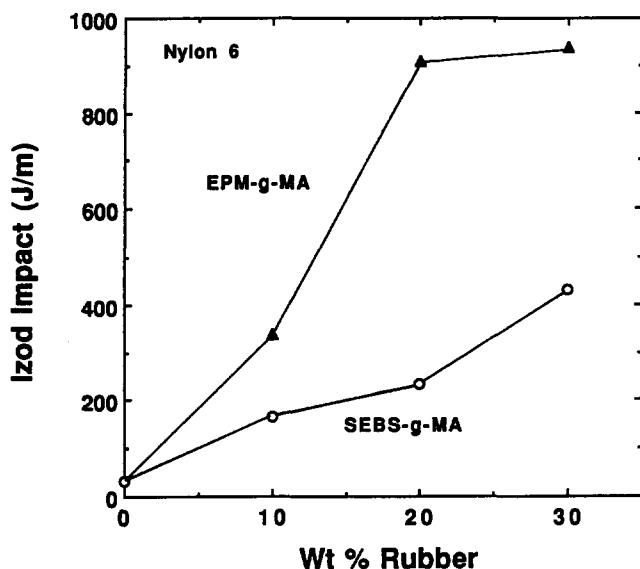


Figure 22 Notched Izod impact strength of nylon-6 blends with SEBS-*g*-MA and with EPM-*g*-MA

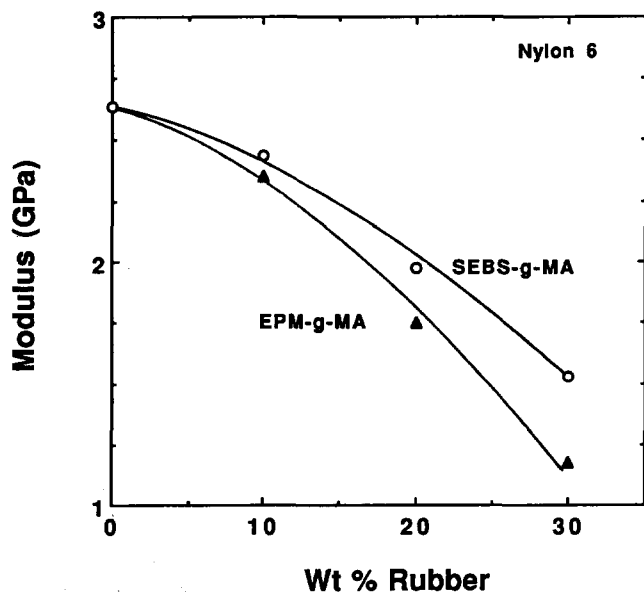


Figure 23 Tensile modulus of nylon-6 blends with SEBS-*g*-MA and with EPM-*g*-MA

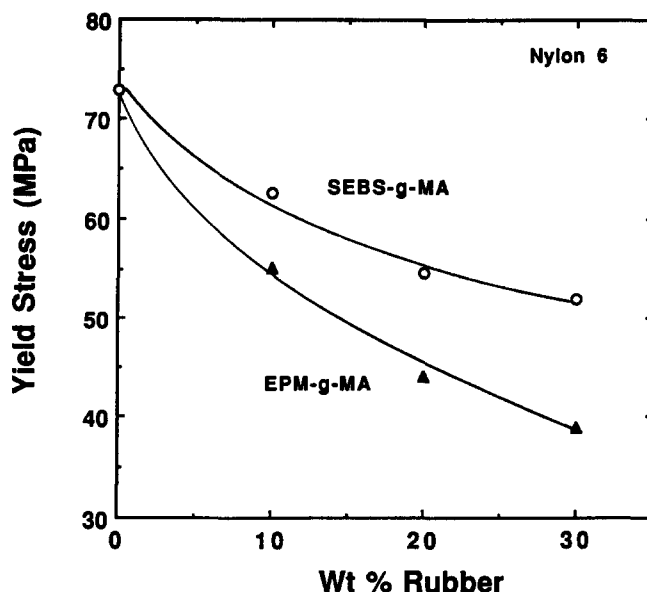


Figure 24 Tensile yield stress of nylon-6 blends with SEBS-*g*-MA and with EPM-*g*-MA

have no similar hard phase. The difference in the yield stress is even more pronounced, as shown in Figure 24.

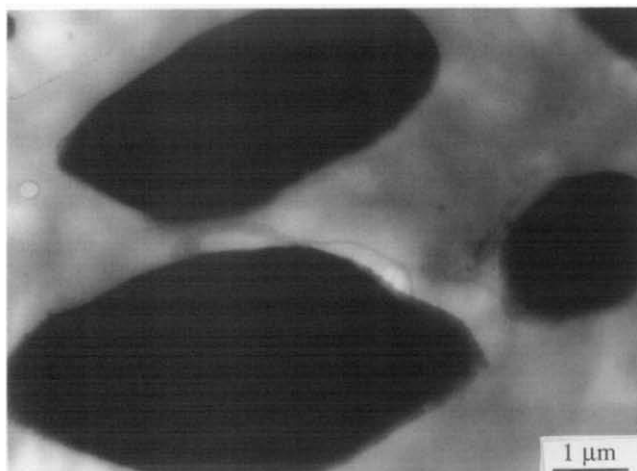
MORPHOLOGY

Some of the reported investigations on rubber toughening of nylons have used scanning electron microscopy (SEM) to characterize the morphology or rubber particle size. However, in the present case SEM techniques were not sufficiently informative so transmission electron microscopy (TEM) was used instead. Because resources to obtain high-quality TEM photomicrographs were limited, only a carefully selected series of specimens, chosen from the materials upon which Figure 14 is based, was examined. The TEM photomicrographs obtained are shown in Figure 25. The letters A–F correspond to the data points so labelled in Figure 14. For pure SEBS, the rubber particles are very large (more than 5 μm in effective diameter) and oblong. As SEBS-*g*-MA is added there is a dramatic reduction in particle size and the particles become progressively more spherical. For pure SEBS-*g*-MA, the mean particle size is about 0.05 μm . In other words, the rubber particle size changes by two orders of magnitude in going from composition A to F.

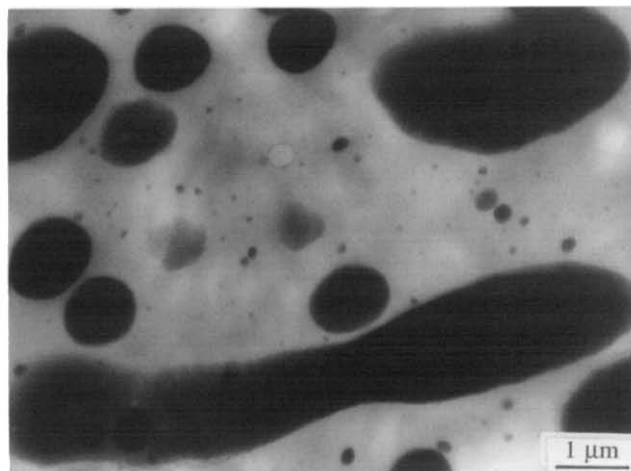
It should be recalled that these blends were prepared by introducing all three components to the extruder simultaneously, and it is of interest to know whether there is a dual population of particles corresponding to each type of rubber or whether the two types of rubber reside more or less uniformly in the same particles. While this issue cannot be determined directly, it is reasonable to expect that the distribution of the particle sizes would be a sensitive indicator. That is, if the two rubbers exist separately in two populations, then there should be a strong bimodality in the particle size distribution owing to the large difference in sizes noted for SEBS and SEBS-*g*-MA individually. Conversely, a unimodal distribution with a varying mean argues for mixing of the two types of rubber.

From simple visual inspection, sample B appears to be bimodal, whereas such behaviour is much less apparent in samples C–E. A more quantitative analysis

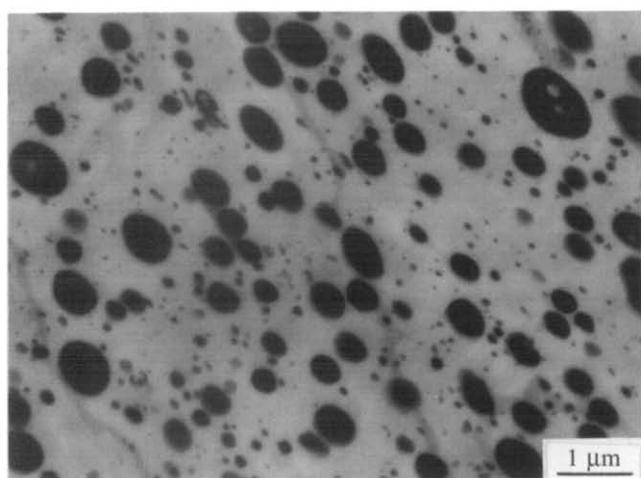
80% Nylon 6 / 20% SEBS (A)



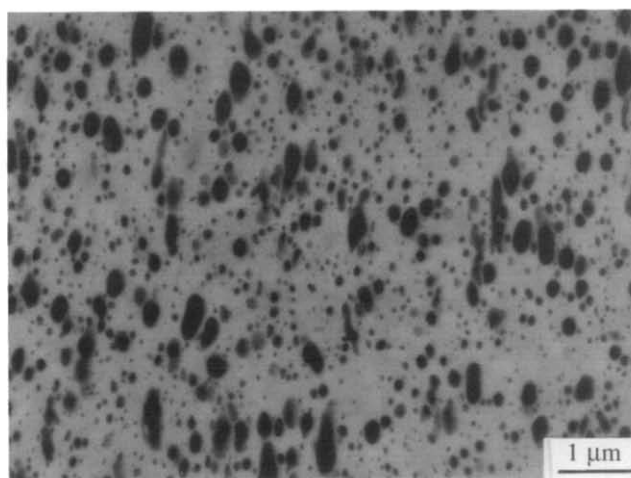
80% Nylon 6 / 18.8% SEBS / 1.2% SEBS-g-MA (B)



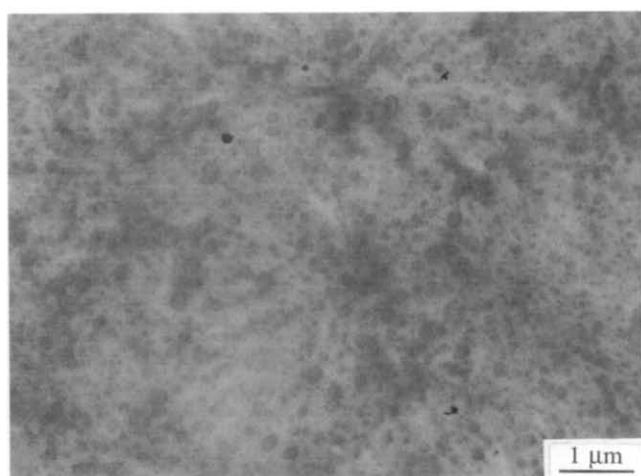
80% Nylon 6 / 16.2% SEBS / 3.8% SEBS-g-MA (C)



80% Nylon 6 / 10% SEBS / 10% SEBS-g-MA (D)



80% Nylon 6 / 4% SEBS / 16% SEBS-g-MA (E)



80% Nylon 6 / 20% SEBS-g-MA (F)

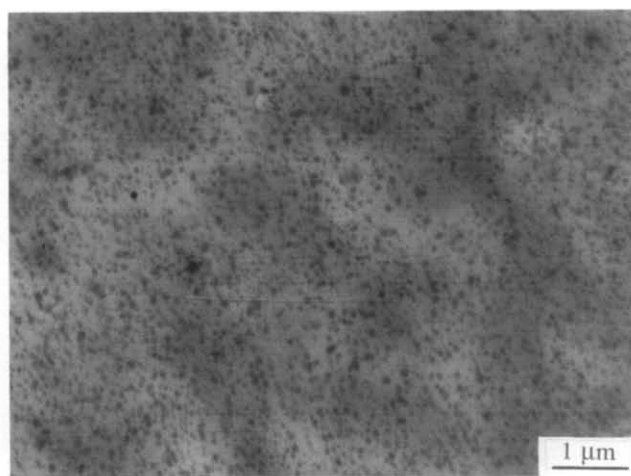


Figure 25 TEM photomicrographs of 20% rubber/80% nylon-6 blends at various ratios of SEBS/SEBS-g-MA rubber. Samples were cryogenically microtomed from injection-moulded bars and stained with OsO_4 and RuO_4

of the size distributions is shown in *Figure 26*. These were obtained by counting particles in *Figure 25* within specified ranges of size to construct the histograms shown. No histogram is shown for sample A since so few particles exist in the field of view. The entire photograph

field was used for samples B and C while only a fraction of the field was used for D to F because of the greater number of particles per unit area. For non-round particles, the area was determined and the diameter of a circle of equivalent area was assigned. Of course, this

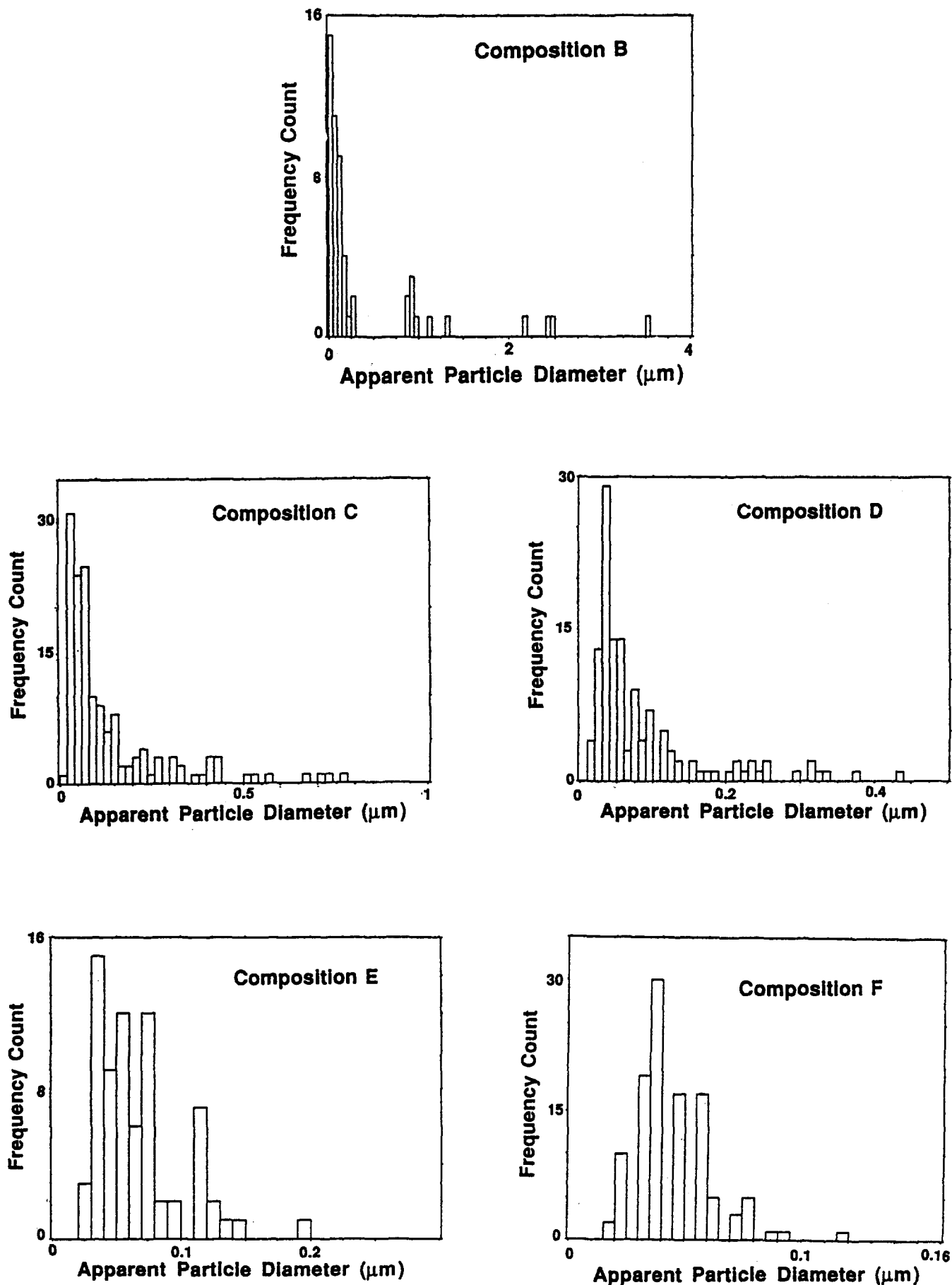


Figure 26 Particle size distributions for 20% rubber/80% nylon-6 blends obtained from the photomicrographs in Figure 25

approach does not take into consideration the fact that the particles are rarely cut through their equators so they appear in two dimensions to be smaller and more broadly distributed in size than they really are. Methods to correct for these effects are known⁴³⁻⁴⁶, but they were not applied here because the limited population of particles sampled did not permit such data manipulations. The histogram for sample B confirms the bimodality apparent by visual inspection. However, none of the other samples show evidence for such bimodality, although the particle size distributions are broad and have a significant tail. These particle size distributions are qualitatively similar to others reported for nylon/rubber blends^{8,18}. In general, we believe these results support a mixed rubber phase or one population of particles. This is quite interesting in view of how the samples were prepared. During the mixing step, the SEBS copolymer must mix with SEBS-*g*-MA simultaneous with a tremendous reduction in particle size of the latter caused by the grafting reaction. Clearly the mixing of the two rubbers may not be complete or perfect. Because of the large ratio of non-functional to functional rubber in composition B and the speed of the graft reaction, it is easy to see how small particles of SEBS-*g*-MA may get formed initially and all the SEBS is not mixed with them in time. This would cause the bimodality shown. No doubt this kind of competition means that the ideal mixing of the two rubbers is only approached but not fully achieved. If the two types of rubber are premixed, before blending with nylon-6, then the opportunity for bimodality or segregation of the two rubbers would seem to be greatly diminished. This point should be explored more carefully in future work with additional TEM analysis. However, from *Table 2* we know that any differences in morphology between samples prepared by these different mixing orders is not enough to influence mechanical properties significantly.

From the quantitative particle size distributions, various average effective particle diameters can be computed. In *Figure 27*, the weight-average particle diameter, defined as:

$$\bar{d}_w = \frac{\sum n_i d_i^2}{\sum n_i d_i}$$

is plotted *versus* the composition of the rubber in the blend. There is a strong decrease in average size up to 20% SEBS-*g*-MA after which the change is less dramatic. It is clear that the increase in Izod impact strength in going from composition A to C is a result of bringing the rubber particle size below the now well recognized^{6,7,18,19,21,25,26} upper limit for effective toughening of nylon-6. Most of the previous papers on toughening nylon-6 have not discussed rubber particles as small as the ones shown in samples E and F. If one postulates a lower limit on particle size for toughening nylon-6 as is suggested for styrenic polymer systems^{5,16,17,47,48}, then this would allow us to explain the decrease in Izod impact strength in going from C to F. In terms of this hypothesis, pure SEBS-*g*-MA is not a particularly effective impact modifier because it produces particles that are too small for effective toughening, and more beneficial results are obtained when it is diluted with SEBS since this raises particle size. Evidently, functionalized ethylene/propylene rubbers do not readily form such small particles; hence, they are

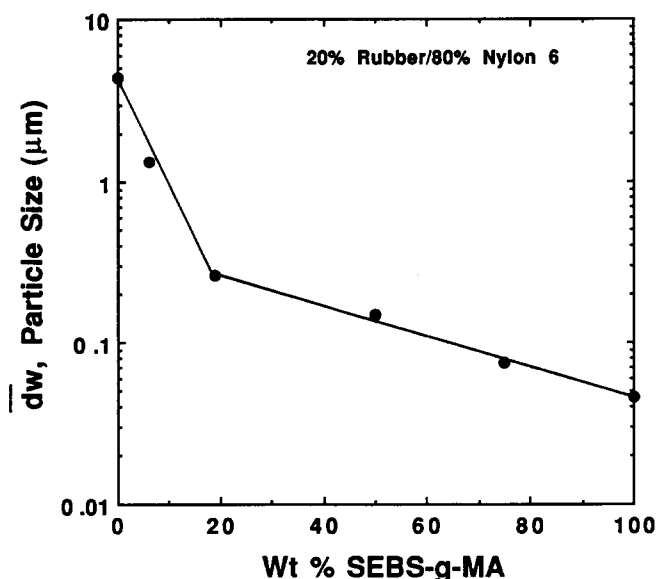


Figure 27 Variation in particle size with SEBS-*g*-MA level for 20% rubber/80% nylon-6 blends

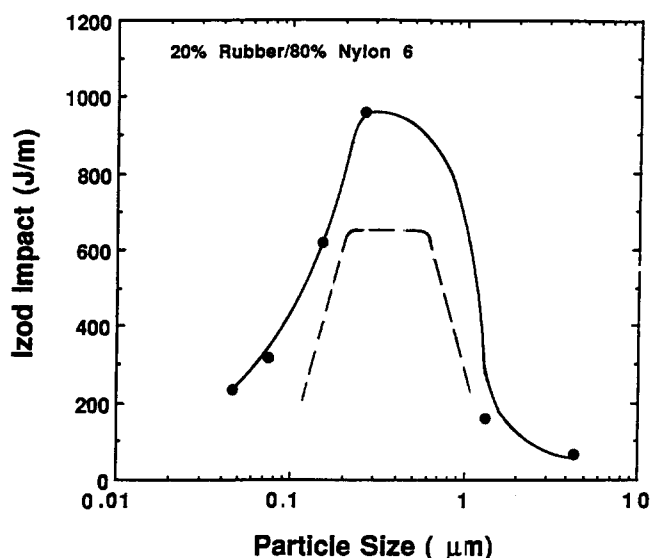


Figure 28 Notched Izod impact strength of 20% rubber/80% nylon-6 blends as a function of particle size. The full curve is drawn by plotting points represented by the lines shown in *Figure 14* and *27*. The broken curve is the one drawn by Gaymans *et al.*³³ through their data for nylon-6

superior to SEBS-*g*-MA for improving impact strength when both are used in the neat form. The differences in particle sizes produced by the two rubbers may relate to the differences in their rheological characteristics.

Very recently Gaymans *et al.*³³ presented similar evidence for a lower limit on particle size for toughening nylon-6 using functionalized ethylene/propylene rubber. They produced particles over a wider size range than reported in their previous work^{7,19,25,26} by varying both functionality and processing conditions. It is interesting to compare their results with ours. The Izod impact strength data from *Figure 14* are replotted in *Figure 28*. The broken curve is the curve Gaymans *et al.*³³ used to represent their data. Their trend is remarkably similar to that of the results reported here. There is some vertical displacement that may partly stem from differences in the geometry of the impact test specimen used by them

compared with those used her. This adds support for the notion of a lower limit on particle size for toughening of nylon-6 and generality since there are significant differences between the two systems. Of course, other factors are also at play, e.g., degree of grafting, morphology of the semicrystalline nylon-6 matrix, etc., in addition to particle size.

INTERFACIAL ADHESION

It is generally recognized that some critical level of adhesion between phases is needed for effective rubber toughening^{5-7,18,19,21,25,26,49}. In many cases, such as hydrocarbon elastomers in polyamides, the level of physical adhesion between such immiscible polymer pairs is not sufficient. One of the premisses for using functionalized elastomers is the formation of chemical bonds across the interface during processing to give improved interfacial adhesion in the solid state. Lap shear adhesion measurements provide a direct means for determining the extent of improvement in adhesion resulting from such reactions^{39,41}. Using the procedure described earlier, the adhesion of nylon-6 to mixtures of SEBS and SEBS-*g*-MA was measured, with the results shown in Figure 29. Each point represents an average of at least seven samples with only interfacial debonding as the cause of specimen failure.

As expected, the adhesion of nylon-6 to SEBS-*g*-MA is significantly greater than that to SEBS, where no chemical bonds can be formed at the interface. However, surprisingly the adhesion does not increase monotonically with SEBS-*g*-MA content of the elastomer phase but there is a maximum in adhesion at about 60% functionalized block copolymer. The number of bonds formed at the interface should be proportional to the amount of SEBS-*g*-MA at the interface and ideally this ought to be proportional to the amount of this component in the elastomer blend. Ordinarily one might expect the level of adhesion to reflect the number of bonds formed; however, there are numerous reasons why this may not be the case. For example, at high levels of anhydride units, extensive surface grafting may lead to local areas of stress concentration and/or brittle material causing an apparent reduction in adhesion. Earlier we

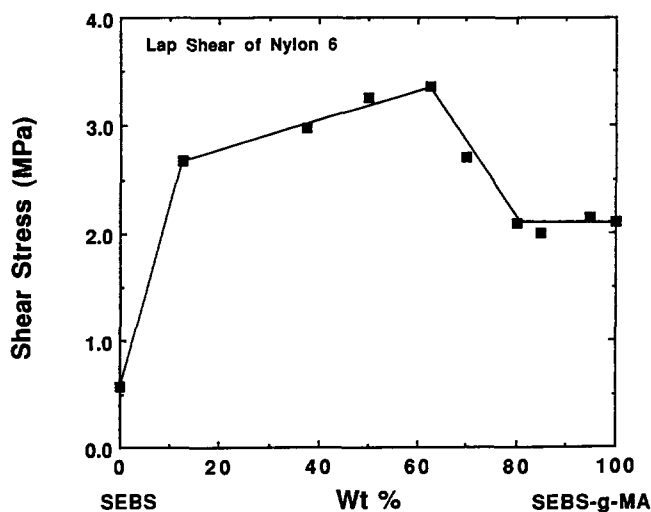


Figure 29 Lap shear adhesive strength of joints between nylon-6 and SEBS/SEBS-*g*-MA blends formed at 240°C for 10 min

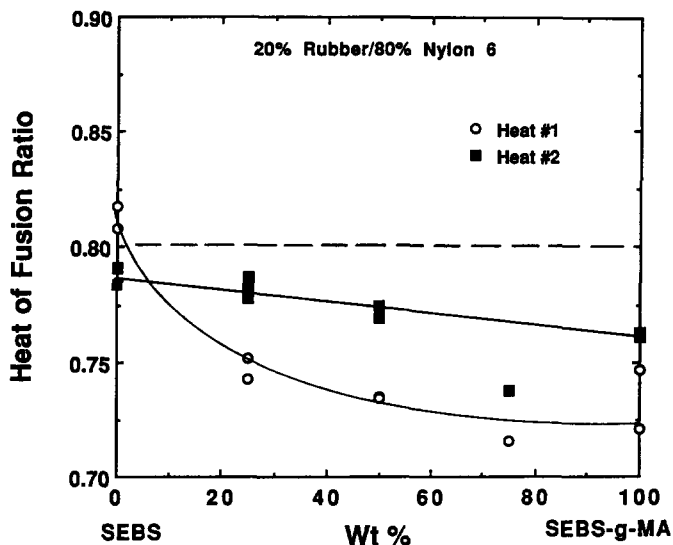


Figure 30 Heat of fusion ratio for injection-moulded 20% rubber/80% nylon-6 blends using d.s.c. Heats of fusion from the first heat for these blends were divided by first heat values of twice extruded nylon-6 ($\Delta H = 61.80 \text{ J g}^{-1}$) and heats of fusion from the second heat were divided by second heat values of twice extruded nylon-6 ($\Delta H = 74.08 \text{ J g}^{-1}$)

showed there is also a maximum in the blend toughness when the SEBS/SEBS-*g*-MA ratio is varied. We hasten to point out that the maximum in adhesion shown in Figure 29 may not be the root cause of this but rather both responses may be the result of issues like that mentioned above. Of course, some analytical assessment of the extent of surface reaction would be helpful in sorting out the cause but such determinations were beyond the scope of this investigation. The main points here, of course, are that functionalization does improve adhesion and that the optimum shown in Figure 29 may reflect micromechanical effects at the interface.

THERMAL AND DYNAMIC MECHANICAL ANALYSIS

While the dispersion of the rubber phase and its coupling to the matrix phase are no doubt dominant issues in the toughening of nylon-6, it must be remembered that the latter is a semicrystalline material whose nature might be changed by the blending process⁵⁰⁻⁵³ and any associated chemistry⁵⁴. First, it is useful to assess the level of nylon-6 crystallinity in selected blends using d.s.c. We focus on the series of blends where the total rubber level is fixed at 20% and the proportions of SEBS and SEBS-*g*-MA are varied (see Figure 14). The heat of fusion found for each blend was divided by that of pure nylon-6 after identical processing, and the results are shown in Figure 30. The absolute value of the peak area for nylon-6 depends on the integration limits used; however, this ratio is relatively insensitive to these limits. If processing did not alter the heat of fusion of the nylon matrix, then all the ratios in Figure 30 should be 0.8 owing to the dilution by the 20% by weight rubber. The first scan reflects the state of the moulded sample and is to some degree influenced by the thermal and mechanical history imposed by the moulding operation, while the second scan is free of this particular history and allows the materials to be compared against a standard thermal history imposed by the d.s.c. protocol. Figure 30 shows

that first scans of all blends containing SEBS-*g*-MA exhibit measurably lower heats of fusion ratios than 0.8. The ratios for these materials are higher on the second heat scans but still less than 0.8. For the blend containing only SEBS type rubber, the ratio is essentially 0.8 after both heats. Multiple points indicate reproducibility using different d.s.c. samples taken from the same moulded bar. From these results one may conclude that the grafting reaction reduces the crystallization rate for nylon-6 and that, as a result, samples with fixed thermal histories, as in the moulding and d.s.c. protocol, have lower levels of nylon-6 crystallinity. Martuscelli *et al.*⁵⁴ have suggested that an elastomeric phase, namely maleic anhydride grafted EPM, reduces the rate of nylon-6 crystallization and therefore reduces the crystallinity achieved, whereas non-functional EPM does not to such an extent.

Figure 31 shows sample d.m.t.a. scans for pure nylon-6 and 20% SEBS-*g*-MA/80% nylon-6. Here we focus on how a few features of the d.m.t.a. results change as the fraction of SEBS-*g*-MA is increased in the series of blends containing 80% nylon-6. First, we note that the storage modulus E' at 25°C decreases rather significantly as the amount of SEBS-*g*-MA increases, as shown in Figure 32. The size of the $\tan \delta$ peak associated with the T_g of nylon-6 (see Table 4) also increases as the blend contains

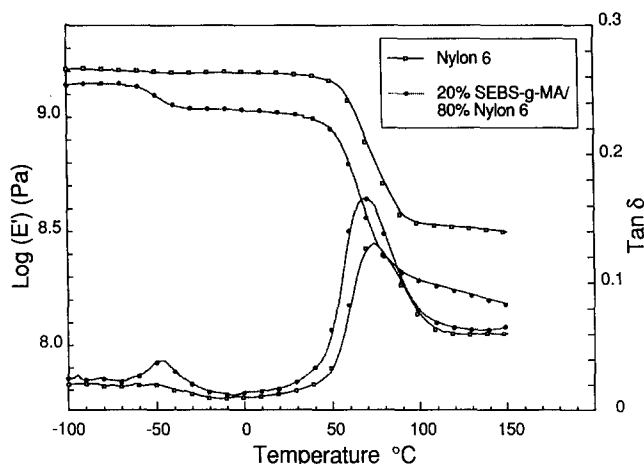


Figure 31 Sample d.m.t.a. scans of pure nylon-6 and a blend containing 20% SEBS-*g*-MA at 1 Hz

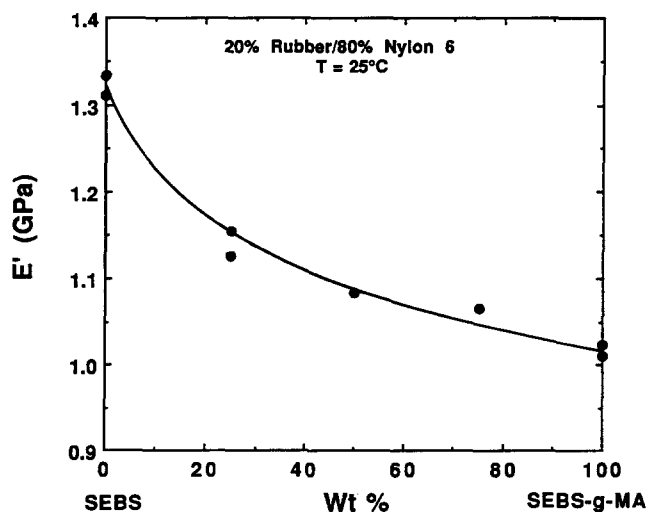


Figure 32 Storage modulus of 20% rubber/80% nylon-6 blends as a function of the amount of SEBS-*g*-MA in the rubber phase

Table 4 Glass transition temperature of rubber phase and nylon-6 matrix in 20% rubber/80% nylon-6 blends from d.m.t.a. at 1 Hz

SEBS- <i>g</i> -MA (wt%)	Rubber $\tan \delta$ peak T_g (°C)	Nylon-6 $\tan \delta$ peak T_g (°C)
Nylon-6 ^a	-51	73
0	-47	71
25	-49	72
50	-49	71
75	-48	73
100	-48	70

^a Nylon-6 was processed at the same conditions as the blends

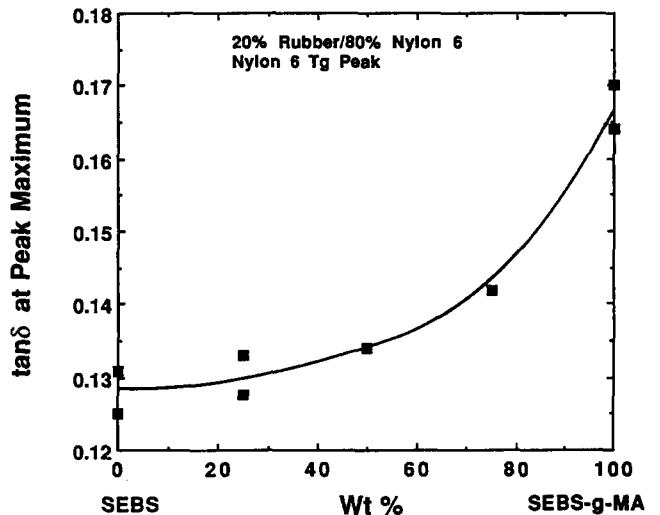


Figure 33 $\tan \delta$ at the nylon-6 glass transition peak maximum for 20% rubber/80% nylon-6 blends as a function of SEBS-*g*-MA in the rubber phase

more SEBS-*g*-MA. This is shown in Figure 33, where the $\tan \delta$ at the maximum for this peak is plotted *versus* the fraction of the rubber in the blend that is SEBS-*g*-MA. The trends in Figure 32 and 33 are consistent with a lower level of crystallinity as found by d.s.c. In addition, there is no doubt some variation in crystalline texture as the graft content is varied.

The nature of the rubber peak in the blends also changes somewhat as the amount of SEBS-*g*-MA is varied, as may be seen from the maximum $\tan \delta$ shown in Figure 34. The damping level seems to decrease as the amount of grafting increases. This effect has been documented for other grafted rubber systems as well^{55,56}.

The changes in the matrix and in the rubber characteristics are significant and need to be considered when discussing the details of the toughening behaviour in this system. However, they are probably not dominant features compared with the tremendous effects of blend morphology described earlier.

CONCLUSIONS

Nylon-6 may be made super-tough by blending with appropriate combinations of SEBS and SEBS-*g*-MA. The order of mixing such ternary compositions in a single-screw extruder does not significantly affect mechanical properties. It appears that the two types of rubber coexist in the same particles, i.e. SEBS-*g*-MA may

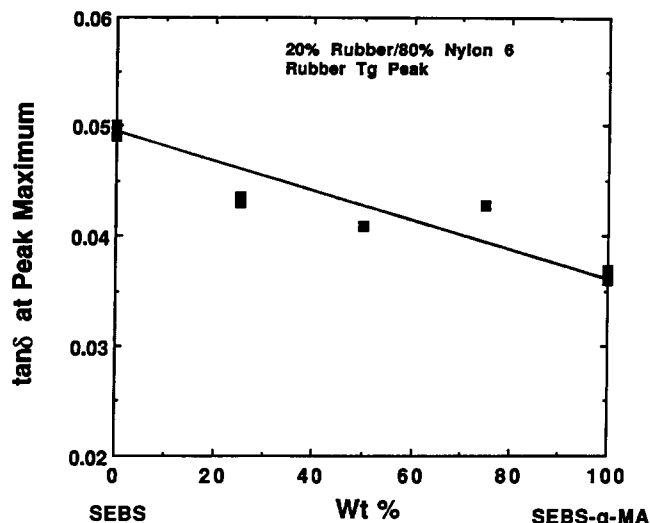


Figure 34 Tan δ at the rubber glass transition peak maximum for 20% rubber/80% nylon-6 blends as a function of SEBS-g-MA in the rubber phase

be said to act as a compatibilizer. By using the two kinds of rubber, particle size was varied by two orders of magnitude using the same melt processing procedure. It is difficult to understand how such large changes can be explained by the usual Taylor drop break-up mechanism^{57,58} simply by the reduction of interfacial tension expected from graft copolymer formation at the domain interfaces. It appears to us that complex rheological forces stemming from the graft reaction may also be part of the mechanism. Of course, grafted chains stabilize particles against coalescence, and this contributes to generation of smaller particles. In addition to the usual maximum rubber particle size for toughening nylon-6, these results support the existence of a minimum rubber particle size that can be effective for toughening nylon-6^{5,33}. Changes in the crystallinity and crystalline texture of the nylon-6 that attend the graft reaction are significant but may not be dominant issues in the toughening mechanism. The graft reaction can be conveniently monitored by melt torque rheometry as demonstrated here. The increase in adhesion caused by these reactions is documented as well.

It is interesting to note that SEBS-g-MA alone is not as effective for toughening nylon-6 as are typical EPM-g-MA elastomers. The reason for this is that SEBS-g-MA forms particles that are too small for effective toughening. We believe that the reasons for this reside in the rheological differences in the two types of rubber. Low-molecular-weight SEBS type materials have low melt viscosity and elasticity compared with the ethylene/propylene copolymers we have examined, which make it easier to disperse the former. The latter apparently has high melt elasticity needed to achieve effective crosslinking behaviour at use temperatures. This feature develops naturally in low-molecular-weight SEBS because of the microphase separation indigenous to the triblock architecture. That is, the thermoplastic elastomeric nature of the block copolymers plays an important role in their behaviour as impact modifiers.

ACKNOWLEDGEMENTS

The research was sponsored by the US Army Research

Office and by the Texas Advanced Technology Program. The authors express their appreciation to Shell Chemical Co. and to COPOLYMER Corp. for donating the elastomers used in this work.

REFERENCES

- Ban, L. L., Doyle, M. J., Disko, M. M. and Smith, G. R. *Polym. Commun.* 1988, **29**, 163
- Lawson, D. F., Hergenrother, W. L. and Matlock, M. G. *J. Appl. Polym. Sci.* 1990, **39**, 2331
- Kinloch, A. J., Shaw, S. J., Tod, D. A. and Hunston, D. L. *Polymer* 1983, **24**, 1341
- Gilmore, D. W. and Modic, M. J. *Plastics Eng.* 1989, April, 29
- Bucknall, C. B. 'Toughened Plastics', Applied Science, London, 1977
- Wu, S. *J. Appl. Polym. Sci.* 1988, **35**, 549
- Borggreve, R. J. M., Gaymans, R. J. and Eichenwald, H. M. *Polymer* 1989, **30**, 78
- Hobbs, S. Y., Bopp, R. C. and Watkins, V. H. *Polym. Eng. Sci.* 1983, **23**, 380
- Jang, B. Z., Uhlmann, D. R. and VanderSande, J. B. *J. Appl. Polym. Sci.* 1984, **29**, 3409
- Margolina, A. and Wu, S. *Polymer* 1988, **29**, 2170
- Sjoerdsma, S. D. *Polymer* 1989, **30**, 106
- Gaymans, R. J. and Dijkstra, K. *Polymer* 1990, **31**, 971
- Wu, S. and Margolina, A. *Polymer* 1990, **31**, 972
- Boyer, R. F. and Keskkula, H. 'Encyclopedia of Science and Technology' (Ed. N. Bikales), Wiley, New York, 1970
- Turley, S. G. and Keskkula, H. *Polymer* 1980, **21**, 466
- Donald, A. M. and Kramer, E. J. *J. Appl. Polym. Sci.* 1982, **27**, 3729
- Keskkula, H. *Adv. Chem. Ser.* **222**, (Ed. Riew, C. K.), Am. Chem. Soc., Washington, DC, 1989, p. 289
- Wu, S. *Polymer* 1985, **26**, 1855
- Borggreve, R. J. M., Gaymans, R. J., Schuijjer, J. and Ingen Housz, J. F. *Polymer* 1987, **28**, 1489
- Epstein, B. N. US Pat. 4 174 358 (to DuPont), 1979
- Wu, S. *Polym. Eng. Sci.* 1987, **27**, 335
- Fayt, R., Jerome, R. and Teyssie, R. *ACS Symp. Ser.* 1989, **395**, 38
- Lambla, M., Yu, R. X. and Lorek, S. *ACS Symp. Ser.* 1989, **385**, 67
- Cimmino, S., Coppola, F., D'Orazio, L., Greco, R., Maglio, G., Malinconico, M., Mancarella, C., Martuscelli, E. and Ragosta, G. *Polymer* 1986, **27**, 1874
- Borggreve, R. J. M. and Gaymans, R. J. *Polymer* 1989, **30**, 63
- Borggreve, R. J. M., Gaymans, R. J. and Schuijjer, J. *Polymer* 1989, **30**, 71
- Legge, N. R., Holden, G. and Schroeder, H. E. (Eds.) 'Thermoplastic Elastomers: A Comprehensive Review', Hanser, New York, 1987
- Modic, M. J., Gilmore, D. W. and Kirkpatrick, J. P. Proc. First Int. Cong. on Compatibilization and Reactive Polymer Alloying (Compalloy '89), New Orleans, LA, 1989, p. 197
- Gelles, B., Modic, M. and Kirkpatrick, J. *Soc. Plast. Eng. ANTEC* 1988, **46**, 513
- Gilmore, D. and Modic, M. *Soc. Plast. Eng., ANTEC* 1989, **47**, 1371
- Greco, R., Malinconico, M., Martuscelli, E., Ragosta, G. and Scarinzi, G. *Polymer* 1987, **28**, 1185
- Cimmino, S., D'Orazio, L., Greco, R., Maglio, G., Malinconico, M., Mancarella, C., Martuscelli, E., Palumbo, R. and Ragosta, G. *Polym. Eng. Sci.* 1984, **24**, 48
- Oostenbrink, A. J., Molenaar, L. J. and Gaymans, R. J. 'Polyamide-Rubber Blends: Influence of Very Small Rubber Particle Sizes on Impact Strength', Poster given at 6th Annual Meeting of Polymer Processing Society, Nice, France, 18-20 April 1990
- Oshinski, A. J., M.S. Thesis, University of Texas at Austin, 1990
- Han, C. D. 'Multiphase Flow in Polymer Processing', Academic Press, New York, 1981
- van Oene, H. in Paul, D. R. and Newman, S. (Eds.) 'Polymer Blends', Vols. I and II, Academic Press, New York, 1978
- Nelson, C. J., Avgeropoulos, G. N., Weissert, F. C. and Bohm, G. G. A. *Angew. Makromol. Chem.* 1977, **60/61**, 49

- 38 Fayt, R., Jerome, R. and Teysse, R. *J. Polym. Sci., Polym. Phys. Edn.* 1984, **22**, 79
- 39 Triacca, V. J., Ziaee, S., Barlow, J. W., Keskkula, H. and Paul, D. R. *Polymer* 1991, **32**, 1401
- 40 Baker, R. E. and Saleem, M. *Polymer* 1987, **28**, 2057
- 41 Barlow, J. W., Shaver, G. P. and Paul, D. R. Proc. First Int. Congr. on Compatibilizers and Reactive Polymer Alloying (Compalloy '89), New Orleans, LA, 1989, p. 221
- 42 Fowler, M. W. and Baker, W. E. *Polym. Eng. Sci.* 1988, **28**, 1427
- 43 Irani, R. R. and Callis, C. F. 'Particle Size: Measurement, Interpretation and Application', Wiley, New York, 1963
- 44 Chamot, E. M. and Mason, C. W. 'Handbook of Chemical Microscopy', Wiley, London, 1983
- 45 Bach, G. 'Qualitative Methods in Morphology', Springer Verlag, Berlin, 1967
- 46 Mihira, K., Ohsawa, T. and Nakayamu, A. *Kolloid. Z.* 1968, **222**, 135
- 47 Donald, A. M. and Kramer, E. J. *J. Mater. Sci.* 1982, **17**, 1765
- 48 Cooper, G. D., Lee, G. F., Katchman, A. and Shank, C. P. *Materials Technology*, Spring 1981, p. 12
- 49 Wu, S. J. *J. Polym. Sci., Polym. Phys. Edn.* 1983, **21**, 699
- 50 Karger-Kocsis, J., Kallo, A., Szafner, A., Bodor, G. and Senyei, Z. *Polymer* 1979, **20**, 37
- 51 Karger-Kocsis, J. and Kulezhev, V.N. *Polymer* 1982, **23**, 699
- 52 Ramsteiner, F., Kanig, G., Heckmann, W. and Gruber, W. *Polymer* 1983, **24**, 365
- 53 Karger-Kocsis, J., Kallo, A. and Kuleznev, V. N. *Polymer* 1984, **25**, 279
- 54 Martuscelli, E., Riva, F., Sellitii, C. and Silvestre, C. *Polymer* 1985, **26**, 270
- 55 Bohn, L. *Angew. Makromol. Chem.* 1971, **20**, 129
- 56 Turley, S. G. *J. Polym. Sci. (C)* 1973, **1**, 101
- 57 Elmendorp, J. J. and Maalcke, R. J. *Polym. Eng. Sci.* 1985, **25**, 1041
- 58 Taylor, G. I. *Proc. R. Soc. Lond. (A)* 1954, **226**, 34